HAROKOPIO UNIVERSITY

→ 4th ADVANCED TRAINING COURSE IN LAND REMOTE SENSING

Optical: Basic Concepts

Jose F. Moreno
University of Valencia, Spain
Jose.Moreno@uv.es

Lecture D2T1b – 2 July 2013

1–5 July 2013 | Harokopio University | Athens, Greece

HAROKOPIO UNIVERSITY

OPTICAL THEORY – BASIC CONCEPTS

- Radiation laws: definitions and nomenclature
- Sources of radiation in natural environment in the optical domain
- Illumination and observation geometries
- Interaction of radiation with matter in the optical domain
- Radiative transfer in the optical domain
- General solutions for the radiation transfer in the coupled Earth-surface and through the atmosphere
- Derivation of surface reflectance from measured satellite radiances
- Spectral information: signatures of natural objects
- Spatial information: uniformity, textures and scales
- Temporal information: land surface dynamics at multiple scales
- Information retrieval: from spectral indices to model inversion
- Overview of applications

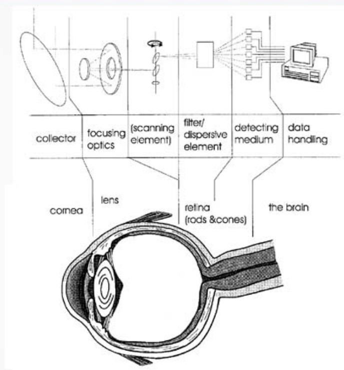

OPTICAL SYSTEMS

Spectral range:
400 - 2500 nm

Panchromatic / Broadband:
one single (broad) band (albedo)

Multispectral	Superspectral	Hyperspectral	Ultraspectral
$1 \lesssim N \lesssim 10$	$10 \lesssim N \lesssim 100$	$100 \lesssim N \lesssim 1000$	$1000 \lesssim N \lesssim ?$
$\Delta\lambda \approx 100$ nm	$\Delta\lambda \approx 50$ nm	$\Delta\lambda \approx 10$ nm	$\Delta\lambda \approx 1$ nm

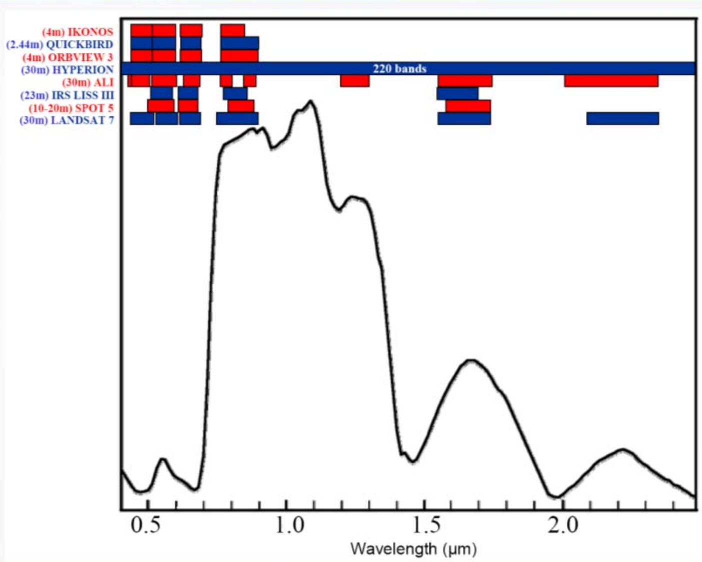

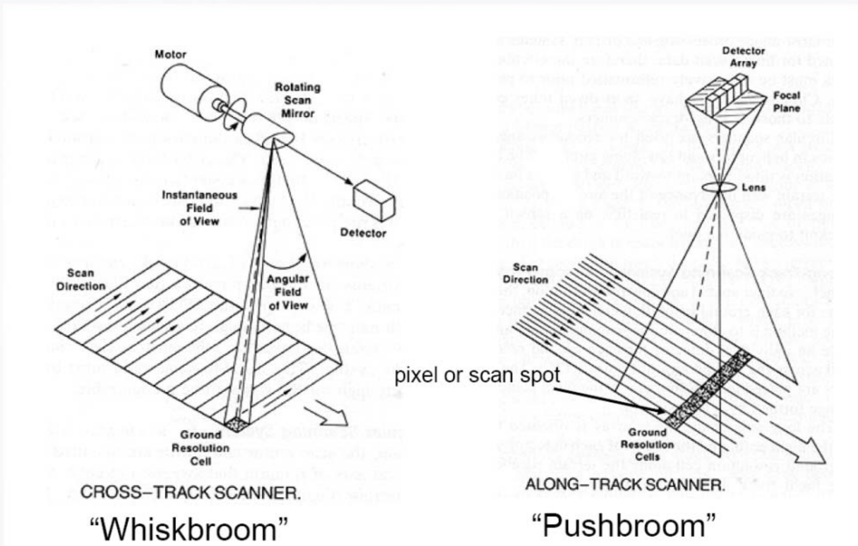

HAROKOPIO UNIVERSITY
esa

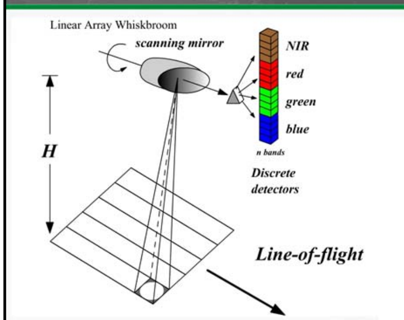

imaging in multiple spectral bands

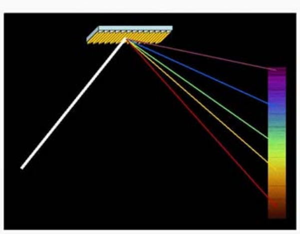

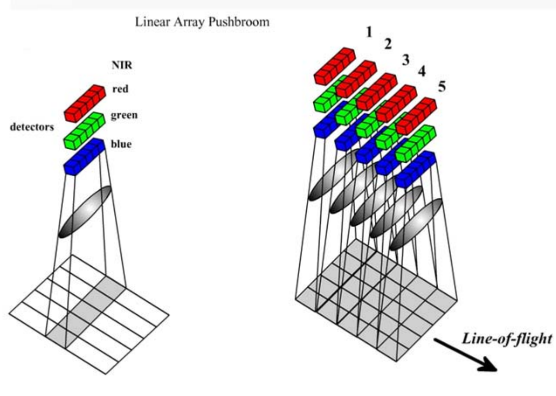

→ 4th ADVANCED TRAINING COURSE IN LAND REMOTE SENSING
1–5 July 2013 | Harokopio University | Athens, Greece

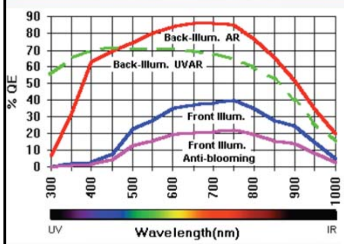

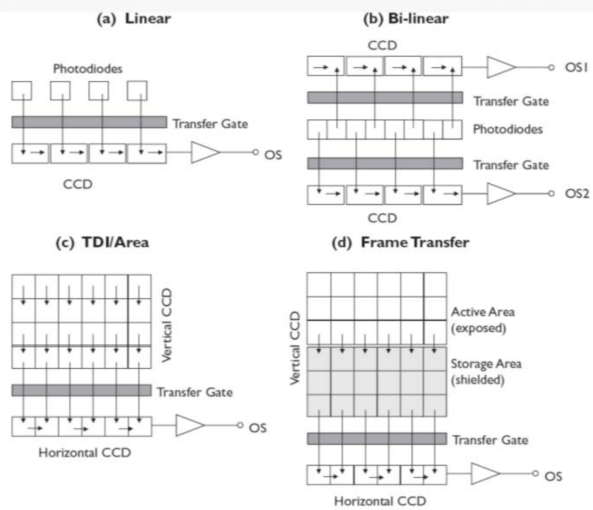

Developments in new sensor technologies

RADIOMETRIC DEFINITIONS

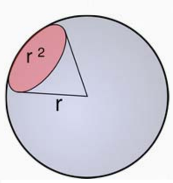

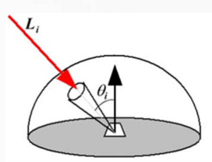

solid angle

$$d\Omega = \frac{(r\ \mathrm{sen}\,\vartheta\ d\varphi)\,(r\ d\vartheta)}{r^2} = \mathrm{sen}\,\vartheta\ d\vartheta\ d\varphi$$

In the particular case of azimuthal symmetry:

$$d\Omega = 2\,\pi\ \mathrm{sen}\,\vartheta\ d\vartheta$$

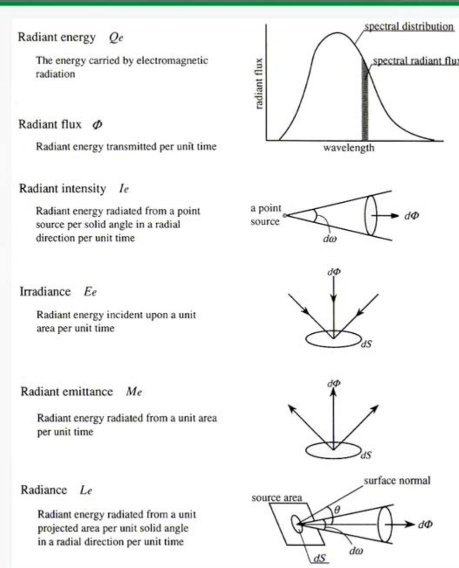

Nomenclature and Radiometric Units

Quantity	Radiometric
Flux	Power (Watts)
Flux/Area	Irradiance (Watts/m^2)
Flux/Solid Angle	Radiant Intensity (Watts/str)
Flux/Area/Solid Angle	Radiance (Watts/m^2/str)

Term or quantity	Unit
Energy content	
radiant energy	joule (J)
energy flow rate	J s^{-1} or watt (W)
energy fluence	J m^{-2}
energy fluence rate	W m^{-2}
Photon content	
number of photons (quanta)	dimensionless
Avogadro's number of photons	mol
photon flow rate	s^{-1} or mol s^{-1}
photon fluence	m^{-2} or mol m^{-2}
photon fluence rate	m^{-2} s^{-1} or mol m^{-2} s^{-1}

RADIANCE

$$L = \frac{d^2\Phi}{d\Omega \ dS} = \frac{d^2\Phi}{d\Omega \ dA \ \cos\vartheta}$$

W m^{-2} sr^{-1}

$$L = \frac{d^3E}{dt \ d\Omega \ dA \ \cos\vartheta}$$

$$M = \int L \cos\vartheta \ d\Omega = \int_0^{2\pi} d\varphi \int_0^{\pi/2} d\vartheta \ L(\vartheta,\varphi) \sin\vartheta \cos\vartheta$$

Lambertian case

$$M = \pi L$$

HAROKOPIO UNIVERSITY

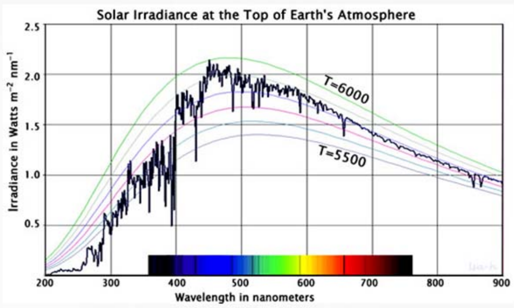

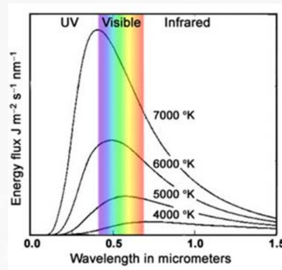

Planck's Law

$$L_\lambda(T) = \frac{2\,h\,c^2}{\lambda^5}\,\frac{1}{e^{\frac{hc}{\lambda kT}} - 1}$$

$c = 299792458 \text{ m s}^{-1}$
$h = 6.62606876\ 10^{-34} \text{ J s}$
$k = 1.3806503\ 10^{-23} \text{ J K}^{-1}$

$\text{W m}^{-2} \text{ sr}^{-1}\ \mu\text{m}^{-1}$

HAROKOPIO UNIVERSITY

Available Signal

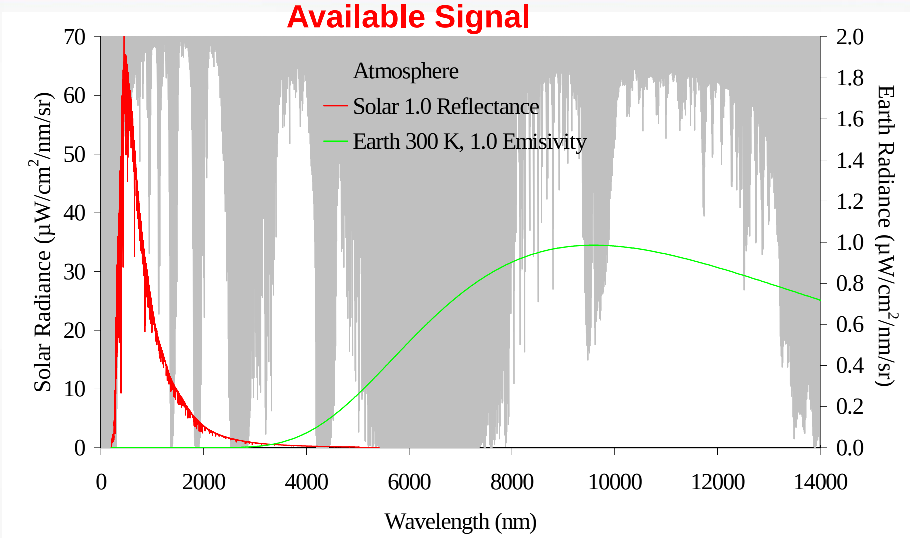

→ 4th ADVANCED TRAINING COURSE IN LAND REMOTE SENSING
1–5 July 2013 | Harokopio University | Athens, Greece

HAROKOPIO UNIVERSITY

Solar irradiance

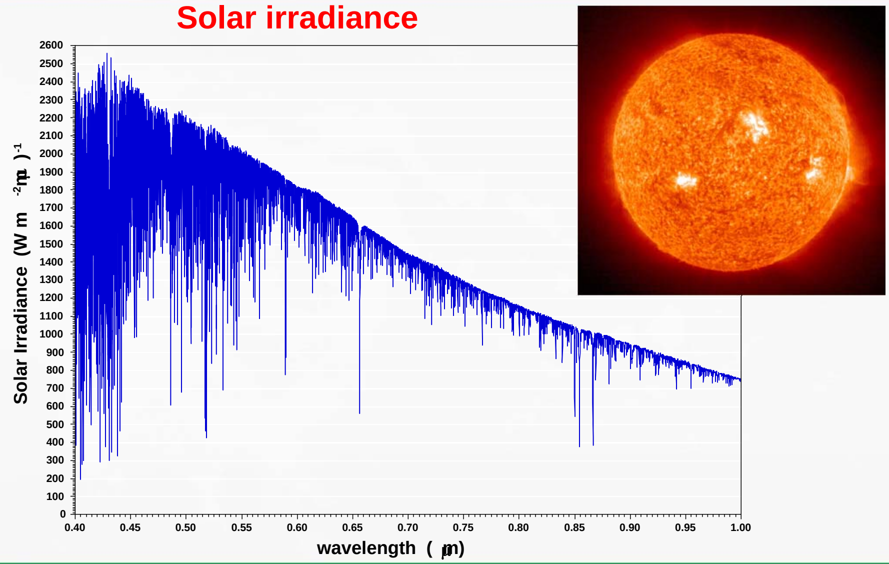

HAROKOPIO UNIVERSITY

simplified model

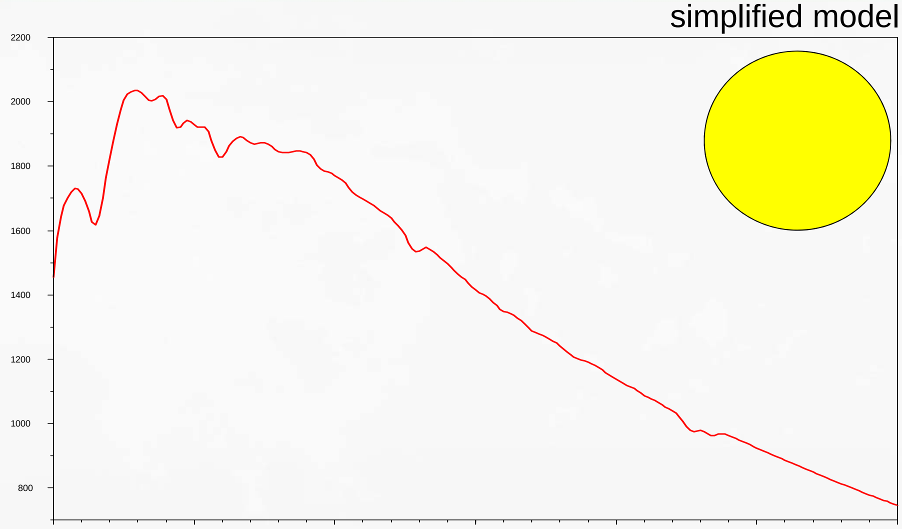

→ 4th ADVANCED TRAINING COURSE IN LAND REMOTE SENSING
1–5 July 2013 | Harokopio University | Athens, Greece

HAROKOPIO UNIVERSITY

esa

Illumination and observation geometries

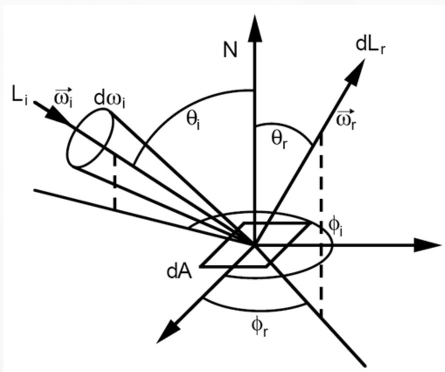

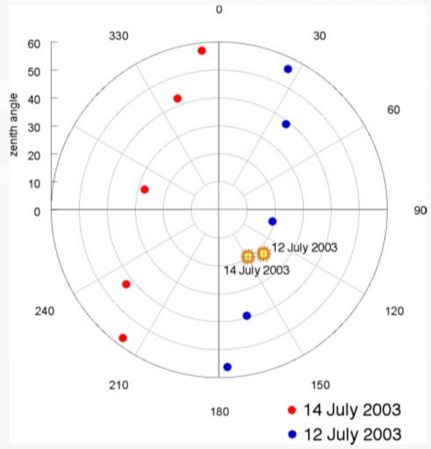

→ 4th ADVANCED TRAINING COURSE IN LAND REMOTE SENSING
1–5 July 2013 | Harokopio University | Athens, Greece

HAROKOPIO UNIVERSITY

esa

Solar and Satellite Orbital Geometry Components

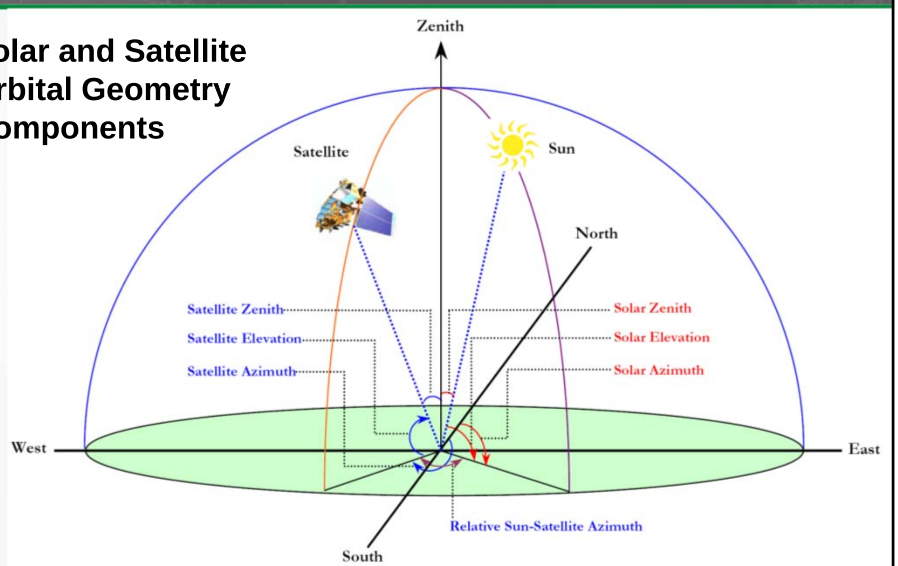

→ 4th ADVANCED TRAINING COURSE IN LAND REMOTE SENSING
1–5 July 2013 | Harokopio University | Athens, Greece

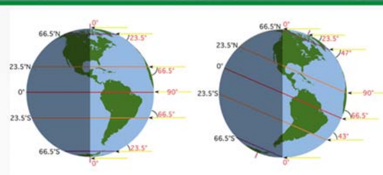
66.5°N
23.5°N
0°
23.5°S
66.5°S
90°

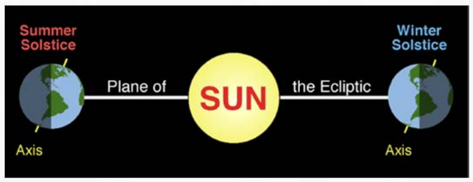
Summer Solstice
Winter Solstice
Plane of
SUN
the Ecliptic
Axis
Axis

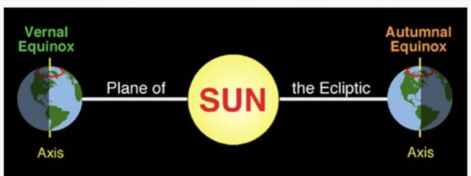
Vernal Equinox
Autumnal Equinox
Plane of
SUN
the Ecliptic
Axis
Axis

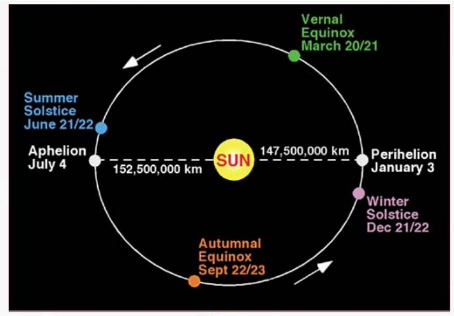
Vernal Equinox March 20/21
Summer Solstice June 21/22
Aphelion July 4
SUN
147,500,000 km
152,500,000 km
Perihelion January 3
Winter Solstice Dec 21/22
Autumnal Equinox Sept 22/23

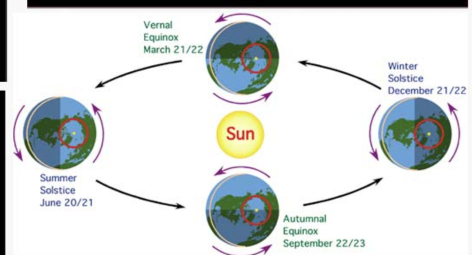
Vernal Equinox March 21/22
Winter Solstice December 21/22
Sun
Summer Solstice June 20/21
Autumnal Equinox September 22/23

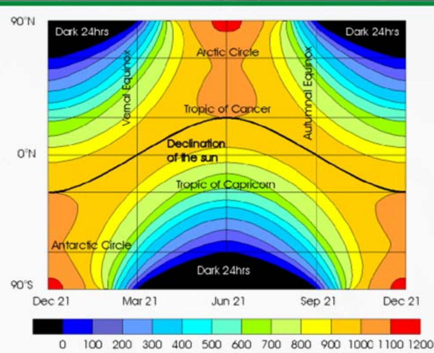
90°N
0°N
90°S
Dark 24hrs
Dark 24hrs
Arctic Circle
Vernal Equinox
Autumnal Equinox
Tropic of Cancer
Declination of the sun
Tropic of Capricorn
Antarctic Circle
Dark 24hrs
Dec 21
Mar 21
Jun 21
Sep 21
Dec 21
0 100 200 300 400 500 600 700 800 900 1000 1100 1200

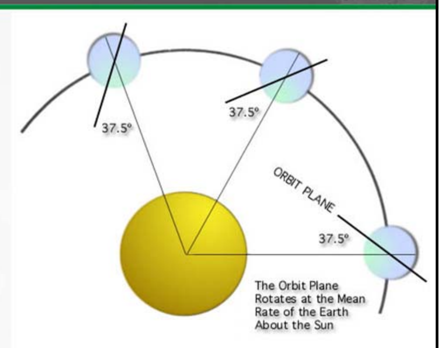
37.5°
37.5°
ORBIT PLANE
37.5°
The Orbit Plane Rotates at the Mean Rate of the Earth About the Sun

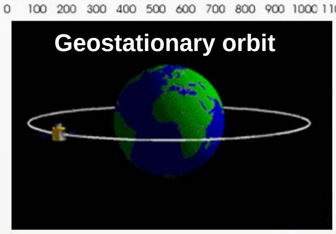
Geostationary orbit

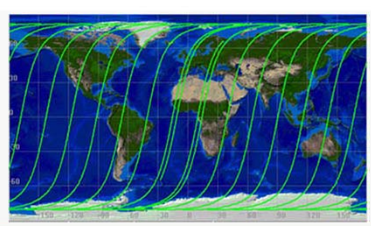

Bidirectional Reflectance Distribution Function, BRDF

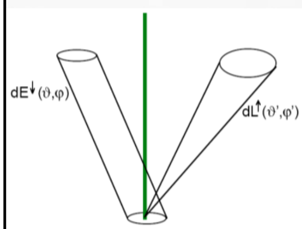

$$f(\vartheta,\varphi,\vartheta',\varphi') = \frac{dL^{\uparrow}(\vartheta',\varphi')}{dE^{\downarrow}(\vartheta,\varphi)}$$

sr^{-1} | $W\ m^{-2}\ sr^{-1}$ | $W\ m^{-2}$

$$f(\vartheta,\varphi,\vartheta',\varphi') = \frac{dL^{\uparrow}(\vartheta',\varphi')}{L^{\downarrow}(\vartheta,\varphi)\cos\vartheta\ \sin\vartheta\ d\vartheta\ d\varphi} = \frac{dL^{\uparrow}(\vartheta',\varphi')}{L^{\downarrow}(\vartheta,\varphi)\cos\vartheta\ d\Omega}$$

- Very difficult to measure experimentally
- Basic tool in computer graphics

Conical Reflectance

$$d\rho(\vartheta,\varphi,\vartheta',\varphi') = \frac{dL^{\uparrow}(\vartheta',\varphi')\cos\vartheta'\ d\Omega'}{L^{\downarrow}(\vartheta,\varphi)\cos\vartheta\ d\Omega}$$

$$d\rho(\vartheta,\varphi,\vartheta',\varphi') = f(\vartheta,\varphi,\vartheta',\varphi')\cos\vartheta'\ d\Omega'$$

Hemispherical Reflectance

$$\rho = \frac{d\Phi^{\uparrow}_{hemisf}}{d\Phi^{\downarrow}_{hemisf}} = \frac{M\ dS}{E\ dS} = \frac{\pi\ L\ dS}{E\ dS} = \frac{\pi\ L}{E}$$

Bidirectional Reflectance Factor

$$R(\vartheta,\varphi,\vartheta',\varphi') = \frac{dL^{\uparrow}_{t}}{dL^{\uparrow}_{p}}$$

nine types of reflectance measurements

	Incident		
Reflected	directional	conical	hemispherical
directional	bidirectional	conical-directional	hemispherical-directional
conical	directional-conical	biconical	hemispherical-conical
hemispherical	directional-hemispherical	conical-hemispherical	bihemispherical

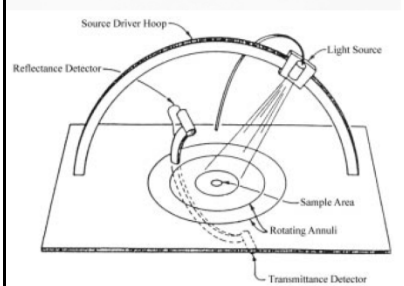

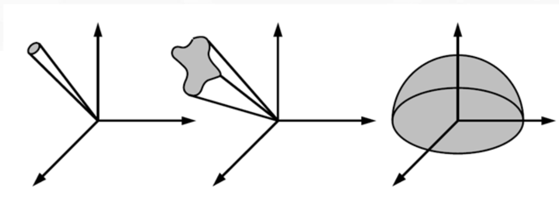

HAROKOPIO UNIVERSITY
esa

Red

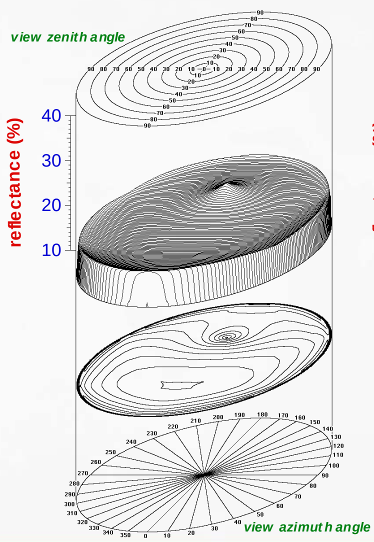

Near-Infrared

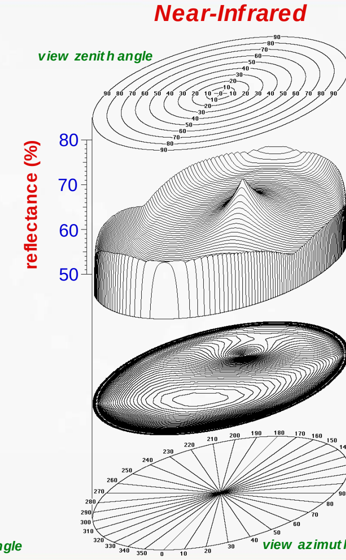

LAI = 4
$\vartheta_{sun} = 35°$
$\varphi_{sun} = 180°$

→ 4th ADVANCED TRAINING COURSE IN LAND REMOTE SENSING
1–5 July 2013 | Harokopio University | Athens, Greece

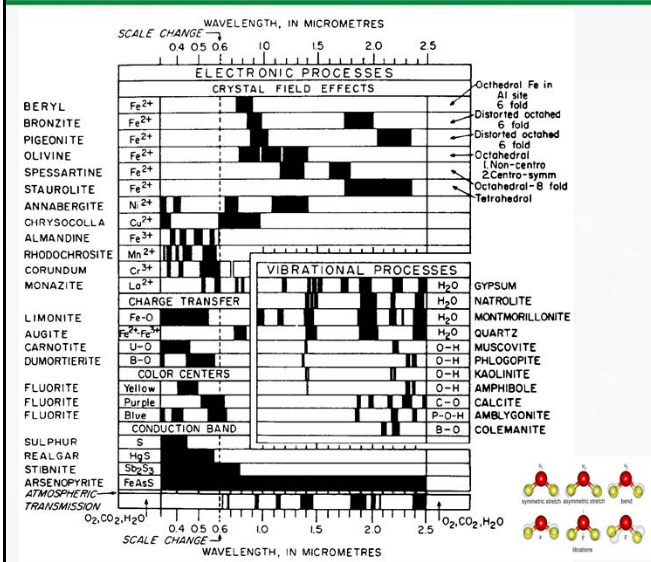

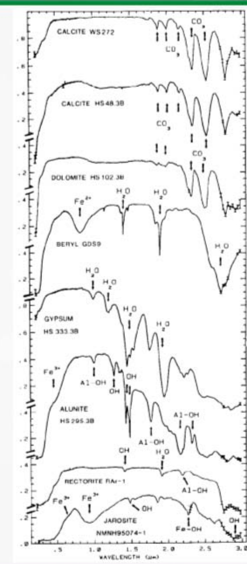

HAROKOPIO UNIVERSITY
esa

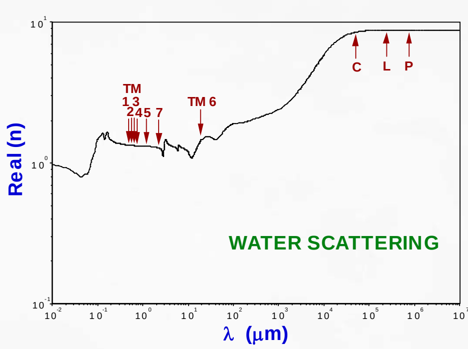

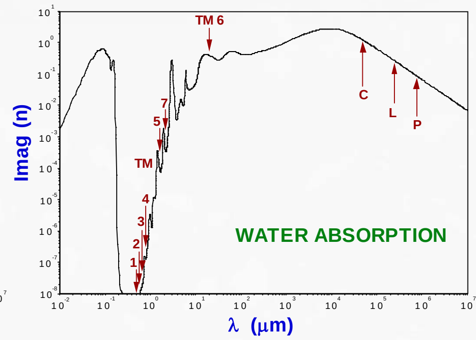

Optical properties of elementary constituents determine the spectral reflectance of land elements

→ 4th ADVANCED TRAINING COURSE IN LAND REMOTE SENSING
1–5 July 2013 | Harokopio University | Athens, Greece

Radiative transfer in the optical domain

$- \beta_a^{ext}(\vec{r},\vec{\Omega})\ \vec{I}(\vec{r},\vec{\Omega})\ dS$

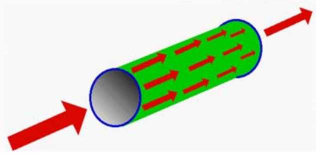

$+ \beta_a^{int}(\vec{r},\vec{\Omega})\ \vec{J}_a(\vec{r},\vec{\Omega})\ dS$

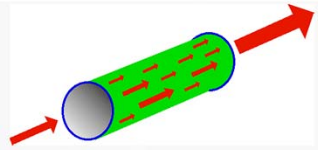

$- \overleftrightarrow{\beta}_s(\vec{r},\vec{\Omega}) \cdot \vec{I}(\vec{r},\vec{\Omega})\ dS$

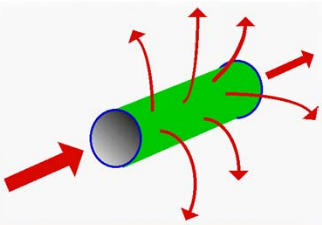

$+ \beta_s(\vec{r},\vec{\Omega})\ \vec{J}_s(\vec{r},\vec{\Omega})\ dS$

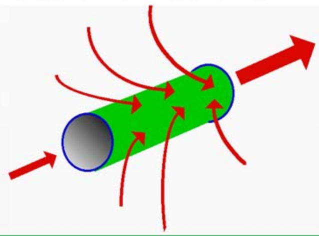

General 5D ([3+2]D) vector radiative transfer equation

$$d\vec{I}(\vec{r},\vec{\Omega}) = - \beta_a^{ext}(\vec{r},\vec{\Omega})\ \vec{I}(\vec{r},\vec{\Omega})\ dS - \overleftrightarrow{\beta}_s(\vec{r},\vec{\Omega}) \cdot \vec{I}(\vec{r},\vec{\Omega})\ dS + $$
$$+ \beta_a^{int}(\vec{r},\vec{\Omega})\ \vec{J}_a(\vec{r},\vec{\Omega})\ dS + \beta_s(\vec{r},\vec{\Omega})\ \vec{J}_s(\vec{r},\vec{\Omega})\ dS$$

$$\vec{J}_s(\vec{r},\vec{\Omega}) = \frac{1}{4\pi} \int_{4\pi} d\vec{\Omega}' \left[\overleftrightarrow{\Psi}_s(\vec{r},\vec{\Omega},\vec{\Omega}') \cdot \vec{I}(\vec{r},\vec{\Omega}') \right]$$

$$\overleftrightarrow{\beta}_s(\vec{r},\vec{\Omega}) = \frac{1}{4\pi} \int_{4\pi} d\vec{\Omega}'\ \overleftrightarrow{\Psi}_s(\vec{r},\vec{\Omega},\vec{\Omega}')$$

… this is most times too complex to be used in practice…

$$\frac{\partial}{\partial s} \equiv \left(\vec{\Omega} \cdot \vec{\nabla}\right)$$

$$\frac{1}{\beta_e(\vec{r},\vec{\Omega})} \frac{\partial}{\partial s} \vec{I}(\vec{r},\vec{\Omega}) = -\vec{I}(\vec{r},\vec{\Omega}) + \frac{\omega_0(\vec{r},\vec{\Omega})}{4\pi} \int_{4\pi} d\vec{\Omega}' \left[\overleftrightarrow{P}(\vec{r},\vec{\Omega},\vec{\Omega}') \cdot \vec{I}(\vec{r},\vec{\Omega}')\right] + \vec{J}(\vec{r},\vec{\Omega})$$

$$d\tau \equiv -\beta_e(\vec{r},\vec{\Omega})\, dz$$

$$d\tau = -\beta_e(\vec{r},\vec{\Omega}) \cos\vartheta\, ds$$

$$ds = \frac{dz}{\cos\vartheta}$$

Signal modelling by multiple contributions

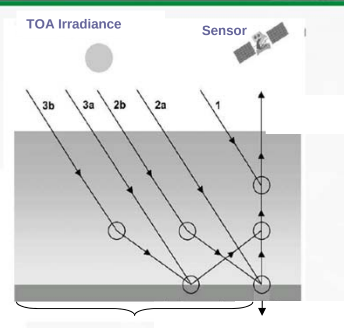

$$\begin{aligned}\rho_{sat} = \rho_{atm} &+ \\ &+ T^{\downarrow} \rho_s T^{\uparrow} + \\ &+ T^{\downarrow} \rho_s S \rho_s T^{\uparrow} + \\ &+ T^{\downarrow} \rho_s S \rho_s S \rho_s T^{\uparrow} + \\ &+ T^{\downarrow} \rho_s S \rho_s S \rho_s S \rho_s T^{\uparrow} + \\ &+ T^{\downarrow} \rho_s S \rho_s S \rho_s S \rho_s S \rho_s T^{\uparrow} + \\ &+ \ldots\end{aligned}$$

HAROKOPIO UNIVERSITY

esa

$$
\begin{aligned}
\rho_{sat} = \rho_{atm} &+ \\
&+ T^{\downarrow}\rho_s T^{\uparrow} + \\
&+ T^{\downarrow}(\rho_s)^2\, S\, T^{\uparrow} + \\
&+ T^{\downarrow}(\rho_s)^3\, S^2\, T^{\uparrow} + \\
&+ T^{\downarrow}(\rho_s)^4\, S^3\, T^{\uparrow} + \\
&+ T^{\downarrow}(\rho_s)^5\, S^4\, T^{\uparrow} + \\
&+ \ldots =
\end{aligned}
$$

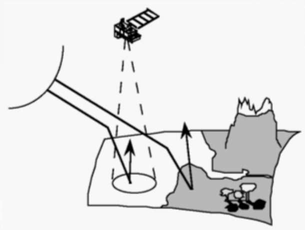

$$= \rho_{atm} + T^{\downarrow}\left[\rho_s + S(\rho_s)^2 + S^2(\rho_s)^3 + S^3(\rho_s)^4 + S^4(\rho_s)^5 + \ldots\right] T^{\uparrow} =$$

$$= \rho_{atm} + T^{\downarrow}\rho_s\left[1 + S\rho_s + S^2(\rho_s)^2 + S^3(\rho_s)^3 + S^4(\rho_s)^4 + \ldots\right] T^{\uparrow} =$$

$$= \rho_{atm} + T^{\downarrow}\rho_s\left[\sum_{n=0}^{\infty}(S\rho_s)^n\right] T^{\uparrow} =$$

$$= \rho_{atm} + T^{\downarrow}\rho_s\left[\frac{1}{1 - S\rho_s}\right] T^{\uparrow}$$

This approximate solution is very useful in practice !!!

→ 4th ADVANCED TRAINING COURSE IN LAND REMOTE SENSING

1–5 July 2013 | Harokopio University | Athens, Greece

HAROKOPIO UNIVERSITY

esa

$$\rho_{sat} = \rho_{atm} + T^{\downarrow}_{dir}\,\check{\hat{\rho}}_s\,T^{\uparrow}_{dir} + T^{\downarrow}_{dir}\,\bar{\check{\rho}}_s\,T^{\uparrow}_{dif} + T^{\downarrow}_{dif}\,\bar{\hat{\rho}}_s\,T^{\uparrow}_{dir} + T^{\downarrow}_{dif}\,\bar{\bar{\rho}}_s\,T^{\uparrow}_{dif}$$

$$
\begin{aligned}
\rho_{sat} = \rho_{atm} &+ \\
&+ T^{\downarrow}_{dir}\,\check{\hat{\rho}}_s\,T^{\uparrow}_{dir} + T^{\downarrow}_{dir}\,\bar{\check{\rho}}_s\,T^{\uparrow}_{dif} + T^{\downarrow}_{dif}\,\bar{\hat{\rho}}_s\,T^{\uparrow}_{dir} + T^{\downarrow}_{dif}\,\bar{\bar{\rho}}_s\,T^{\uparrow}_{dif} + \\
&+ T^{\downarrow}_{dir}\,\bar{\check{\rho}}_s\,S\,\bar{\hat{\rho}}_s\,T^{\uparrow}_{dir} + T^{\downarrow}_{dir}\,\bar{\check{\rho}}_s\,S\,\bar{\bar{\rho}}_s\,T^{\uparrow}_{dif} + T^{\downarrow}_{dif}\,\bar{\bar{\rho}}_s\,S\,\bar{\hat{\rho}}_s\,T^{\uparrow}_{dir} + T^{\downarrow}_{dif}\,\bar{\bar{\rho}}_s\,S\,\bar{\bar{\rho}}_s\,T^{\uparrow}_{dif} + \\
&+ T^{\downarrow}_{dir}\,\bar{\check{\rho}}_s\,S\,\bar{\bar{\rho}}_s\,S\,\bar{\hat{\rho}}_s\,T^{\uparrow}_{dir} + T^{\downarrow}_{dir}\,\bar{\check{\rho}}_s\,S\,\bar{\bar{\rho}}_s\,S\,\bar{\bar{\rho}}_s\,T^{\uparrow}_{dif} + T^{\downarrow}_{dif}\,\bar{\bar{\rho}}_s\,S\,\bar{\bar{\rho}}_s\,S\,\bar{\hat{\rho}}_s\,T^{\uparrow}_{dir} + \\
&\qquad + T^{\downarrow}_{dif}\,\bar{\bar{\rho}}_s\,S\,\bar{\bar{\rho}}_s\,S\,\bar{\bar{\rho}}_s\,T^{\uparrow}_{dif} + \\
&+ T^{\downarrow}_{dir}\,\bar{\check{\rho}}_s\,S\,\bar{\bar{\rho}}_s\,S\,\bar{\bar{\rho}}_s\,S\,\bar{\hat{\rho}}_s\,T^{\uparrow}_{dir} + T^{\downarrow}_{dir}\,\bar{\check{\rho}}_s\,S\,\bar{\bar{\rho}}_s\,S\,\bar{\bar{\rho}}_s\,S\,\bar{\bar{\rho}}_s\,T^{\uparrow}_{dif} + \\
&\qquad + T^{\downarrow}_{dif}\,\bar{\bar{\rho}}_s\,S\,\bar{\bar{\rho}}_s\,S\,\bar{\bar{\rho}}_s\,S\,\bar{\hat{\rho}}_s\,T^{\uparrow}_{dir} + T^{\downarrow}_{dif}\,\bar{\bar{\rho}}_s\,S\,\bar{\bar{\rho}}_s\,S\,\bar{\bar{\rho}}_s\,S\,\bar{\bar{\rho}}_s\,T^{\uparrow}_{dif} + \\
&+ \ldots\ldots =
\end{aligned}
$$

→ 4th ADVANCED TRAINING COURSE IN LAND REMOTE SENSING

1–5 July 2013 | Harokopio University | Athens, Greece

SATELLITE SIGNAL MODELLING

$$\rho'(\theta_s,\theta_v,\phi_v) = t_g(\theta_s,\theta_v)\,\{\rho_a(\theta_s,\theta_v,\phi_v) + \frac{T(\theta_s)}{1-<\rho(M)>S}[\rho_c(M)e^{-\tau/\mu_v} + <\rho(M)>t_d(\theta_v)]\}$$

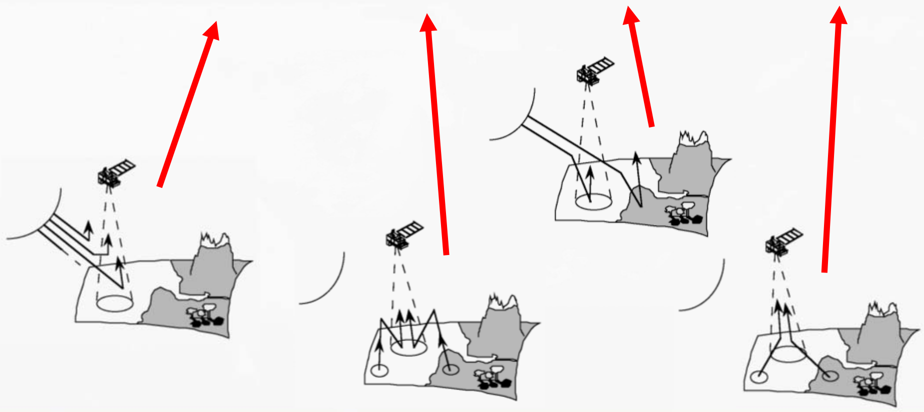

HAROKOPIO UNIVERSITY
esa

Pre-processing steps:

- Radiometric calibration
- Noise removal
- Cloud screening
- Geometric correction
- Atmospheric correction
- Data integration

4th ADVANCED TRAINING COURSE IN LAND REMOTE SENSING
1–5 July 2013 | Harokopio University | Athens, Greece

RADIOMETRIC CALIBRATION

- Pre-launch radiometric calibration to traceable standard (accepted reference)
- Post launch calibration campaigns to maintain/monitoring in flight calibration (vicarious)
- On-board calibration (both radiometric and spectral)

HAROKOPIO UNIVERSITY
esa

CLOUD SCREENING

- Very dependent on the available spectral information
- Many different algorithms (from simple thresholds up to sophisticate techniques)

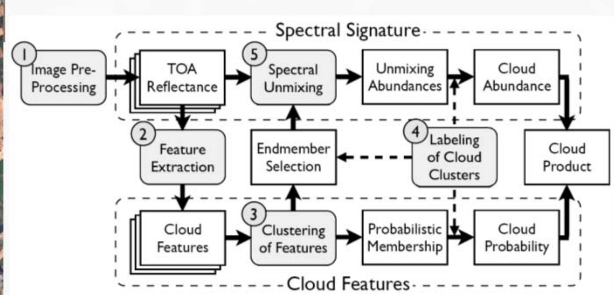

→ 4th ADVANCED TRAINING COURSE IN LAND REMOTE SENSING
1–5 July 2013 | Harokopio University | Athens, Greece

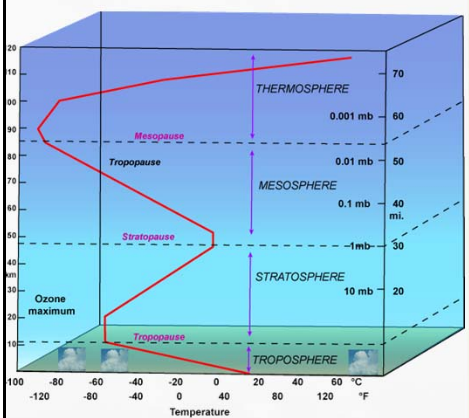

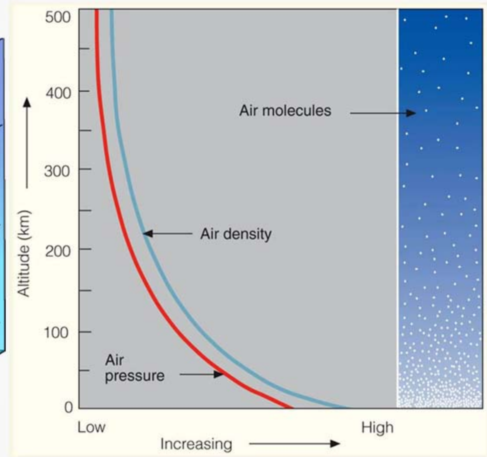

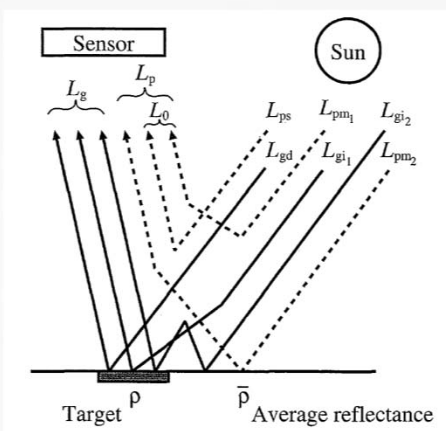

- The atmosphere modifies the radiation measured by optical sensors:
- Aerosols and gases present optical activity at VIS/NIR/SWIR.
- Reflectance increases/decreases depending on the wavelength.
- Image loses contrast.

→ Removing the atmospheric influence from remote sensing data is necessary before the data exploitation

Surface reflectance retrieval

- TOA radiance modeled assuming Lambertian reflectance for the target:

$$L_{\mathrm{TOA}} = L_0 + \frac{1}{\pi}\frac{\rho_s(E_{\mathrm{dir}}\mu_{\mathrm{il}} + E_{\mathrm{dif}})T_{\uparrow}}{1 - S\rho_s}$$

- Analytically invertible to retrieve ρ_s.

$$\rho_s = \frac{L_{\mathrm{TOA}} - L_0}{[(E_{\mathrm{dir}}\mu_{\mathrm{il}} + E_{\mathrm{dif}})\frac{T_{\uparrow}}{\pi}] + S[L_{\mathrm{TOA}} - L_0]}$$

- Removal of adjacency effects

INVERSION OF SURFACE REFLECTANCE

Flat Lambertian areas:

$$\rho' = A + \frac{B\,\rho_c + C <\rho>}{1 - S <\rho>}$$

$$\rho_c = \frac{\left(\frac{\rho' - A}{B}\right) - \frac{C}{B + C}\left(\frac{<\rho'> - A}{B}\right)}{1 + S\,\frac{B}{B + C}\left(\frac{<\rho'> - A}{B}\right)}$$

Non-Lambertian areas with topographic structure:

- no analytic inversion under approximations
- decoupling 'effective' reflectances and 'effective' geometric terms required for environment
- multistep numerical procedure required for inversion
- multiple reflection terms only significant for high reflectance surroundings

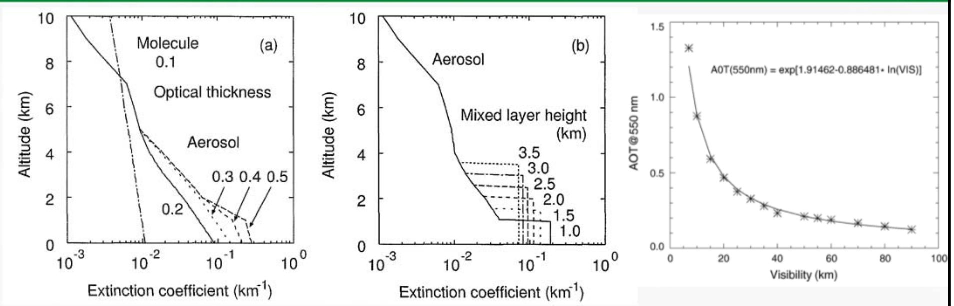

Permanent Constituents		Variable constituents	
Constituent	% by volume	Constituent	% by volume
Nitrogen (N_2)	78.084	Water Vapor (H_2O)	0.04
Oxygen (O_2)	20.948	Ozone (O_3)	12×10^{-4}
Argon (Ar)	0.934	Sulfur dioxide (SO_2)[b]	0.001×10^{-4}
Carbon dioxide (CO_2)	0.033	Nitrogen dioxide (NO_2)	0.001×10^{-4}
Neon (Ne)	18.18×10^{-4}	Ammonia (NH_3)	0.001×10^{-4}
Helium (He)	5.24×10^{-4}	Nitric oxide (NO)	0.0005×10^{-4}
Krypton (Kr)	1.14×10^{-4}	Hydrogen sulfide (H_2S)	0.00005×10^{-4}
Xenon (Xe)	0.089×10^{-4}	Nitric acid vapor	trace
Hydrogen (H_2)	0.5×10^{-4}		
Methane (CH_4)	1.5×10^{-4}		
Nitrous Oxide (N_2O)	0.27×10^{-4}		
Carbon Monoxide (CO)	0.19×10^{-4}		

HAROKOPIO UNIVERSITY

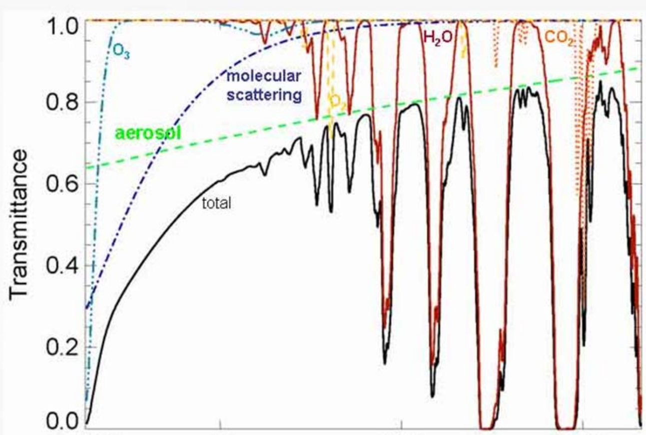

→ 4th ADVANCED TRAINING COURSE IN LAND REMOTE SENSING
1–5 July 2013 | Harokopio University | Athens, Greece

HAROKOPIO UNIVERSITY

Surface reflectance retrieval

Atmospheric correction: Removal of the atmospheric effects from the measured at-sensor radiance, leading to the derivation of surface reflectance images.

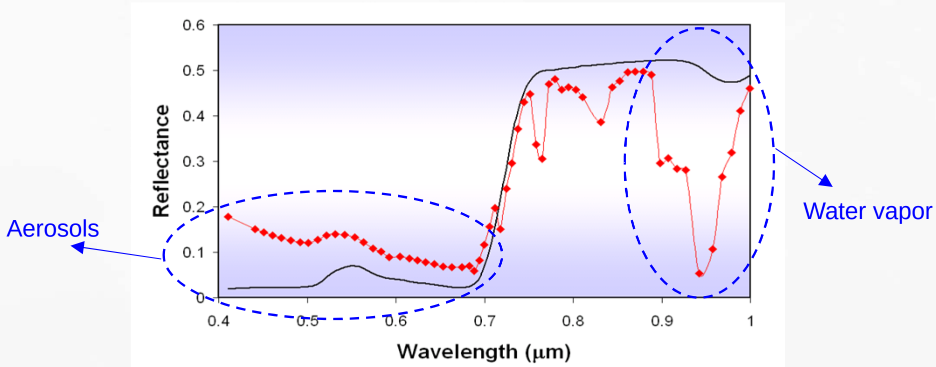

→ 4th ADVANCED TRAINING COURSE IN LAND REMOTE SENSING
1–5 July 2013 | Harokopio University | Athens, Greece

HAROKOPIO UNIVERSITY

ATMOSPHERIC INFORMATION

In-situ radiosoundings

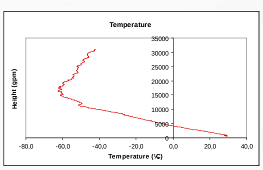

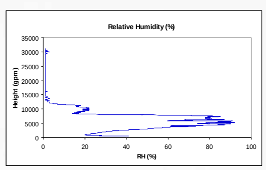

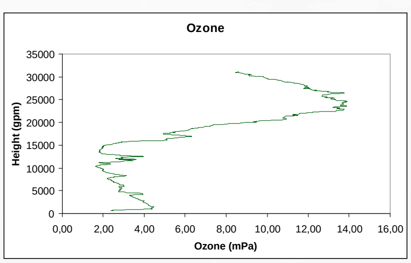

In-situ spectral irradiance

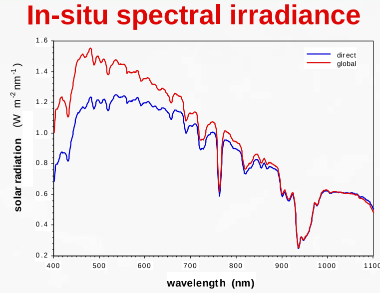

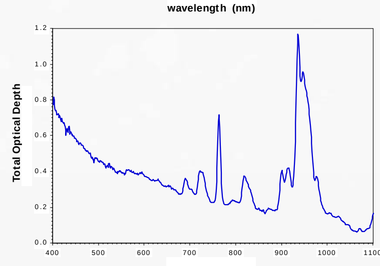

→ 4th ADVANCED TRAINING COURSE IN LAND REMOTE SENSING
1–5 July 2013 | Harokopio University | Athens, Greece

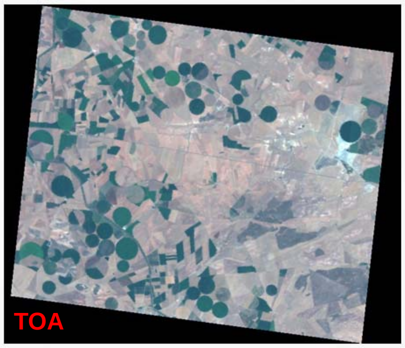

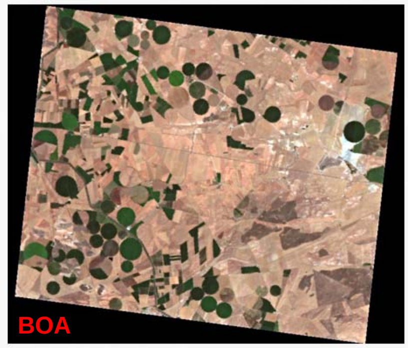

HAROKOPIO UNIVERSITY

Topographic effects

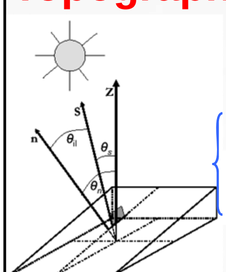

$$L_{TOA} = L_0 + \frac{1}{\pi}\frac{\rho_s(E_{dir}\mu_{il} + E_{dif})T\uparrow}{1 - S\rho_s}$$

$$\mu_{il} = \mathbf{n}\cdot\mathbf{S}$$

→ Cosine correction

$$E^t_{dif}(x,y,z) = E_{dif}(z)\left[t_{dir}(z)\mu_{il}(x,y) + [1 - t_{dir}(z)\mu_s]\frac{1+\mu_n(x,y)}{2}\right]$$

→ Hay's model

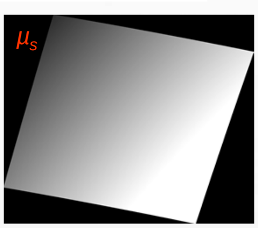

+

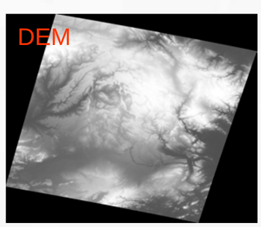

=

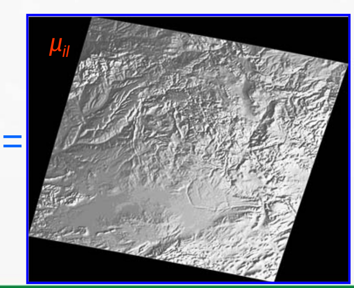

→ 4th ADVANCED TRAINING COURSE IN LAND REMOTE SENSING
1–5 July 2013 | Harokopio University | Athens, Greece

HAROKOPIO UNIVERSITY

BRDF effects

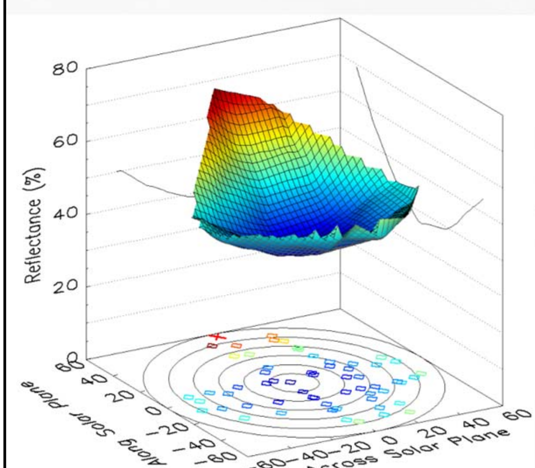

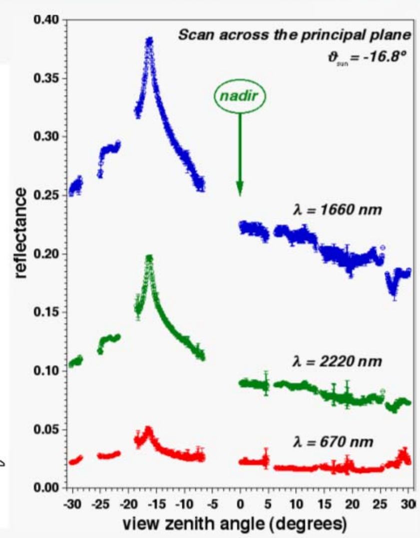

→ 4th ADVANCED TRAINING COURSE IN LAND REMOTE SENSING
1–5 July 2013 | Harokopio University | Athens, Greece

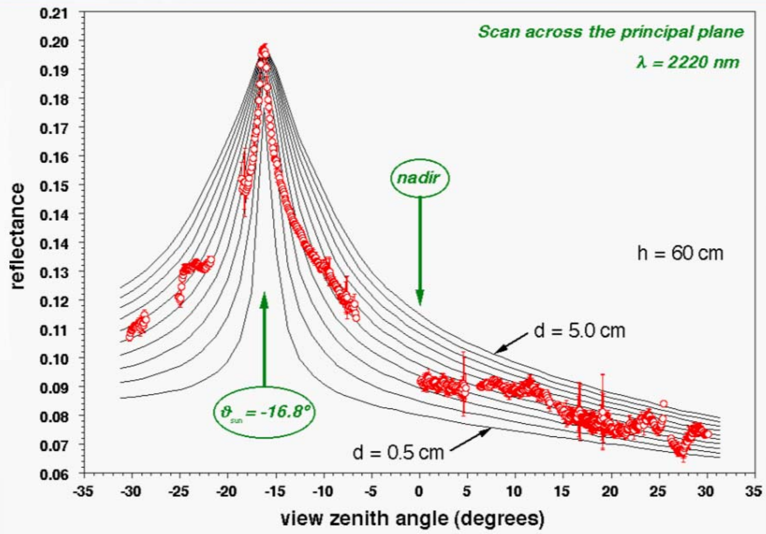

HAROKOPIO UNIVERSITY
esa

CHRIS/PROBA satellite view angles

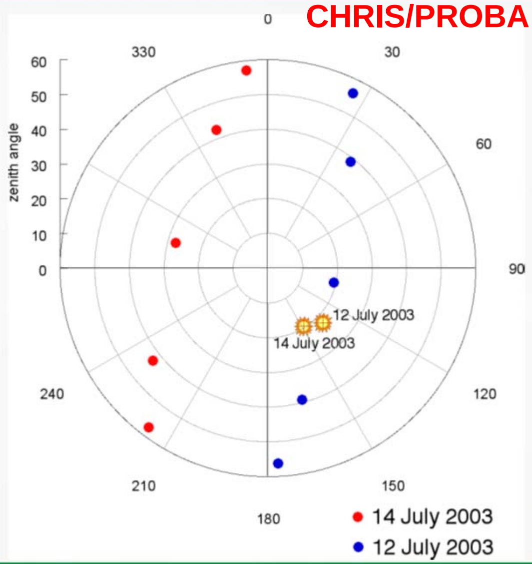

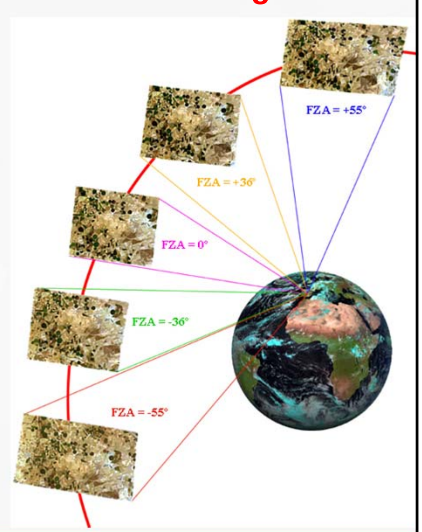

→ 4th ADVANCED TRAINING COURSE IN LAND REMOTE SENSING
1–5 July 2013 | Harokopio University | Athens, Greece

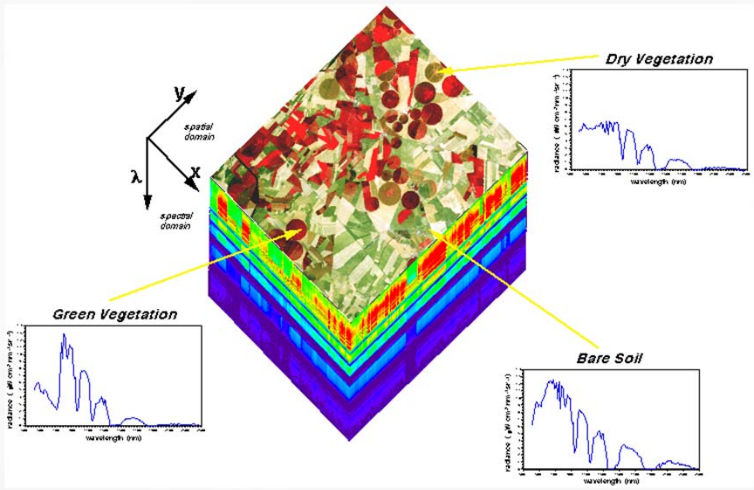

HAROKOPIO UNIVERSITY
esa

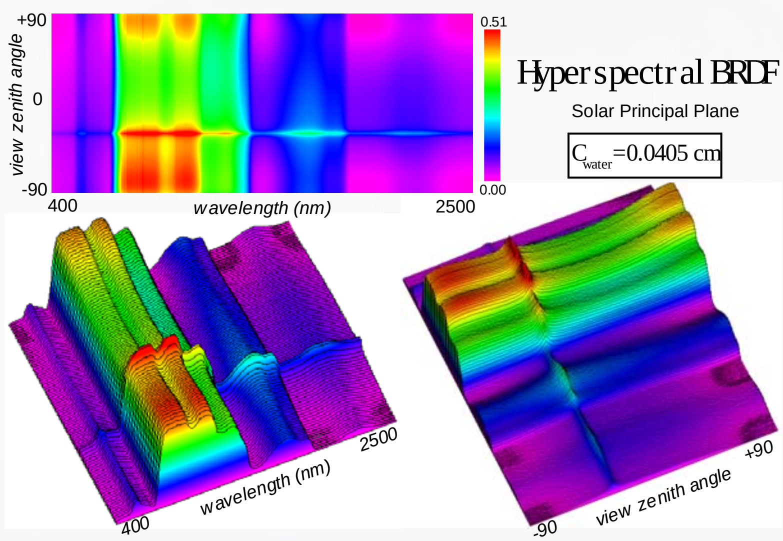

→ 4th ADVANCED TRAINING COURSE IN LAND REMOTE SENSING
1–5 July 2013 | Harokopio University | Athens, Greece

SOIL REFLECTANCE

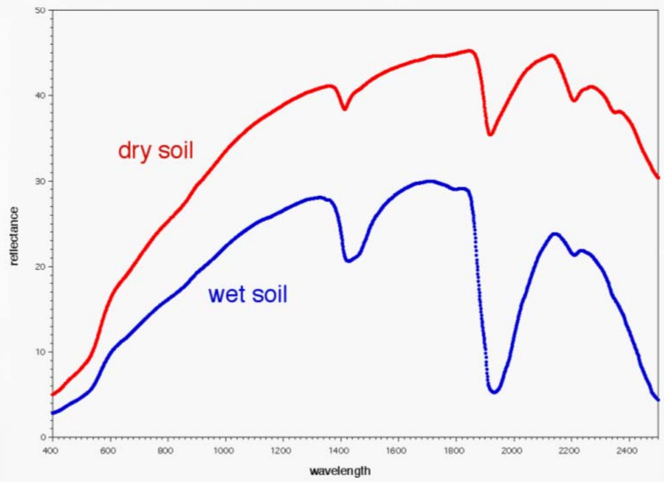

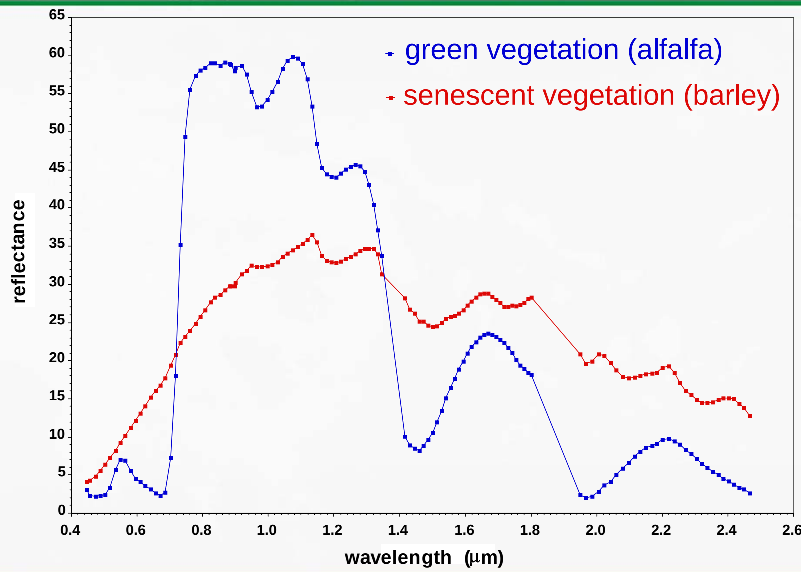

HAROKOPIO UNIVERSITY

esa

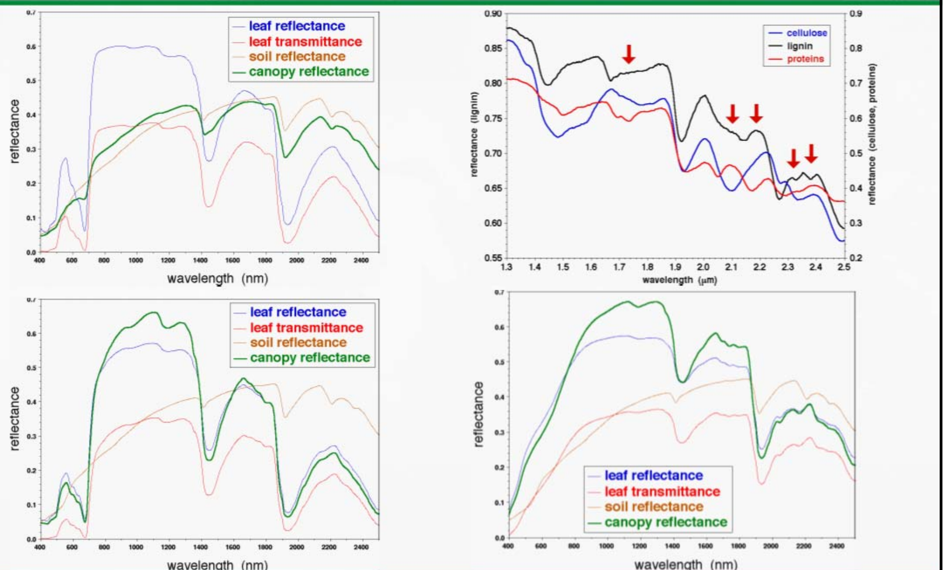

→ 4th ADVANCED TRAINING COURSE IN LAND REMOTE SENSING
1–5 July 2013 | Harokopio University | Athens, Greece

HAROKOPIO UNIVERSITY

esa

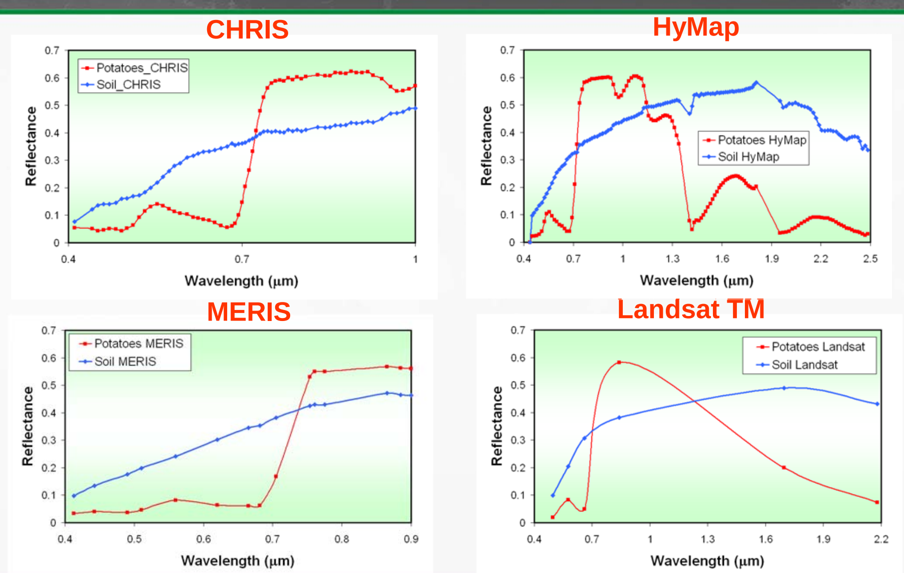

→ 4th ADVANCED TRAINING COURSE IN LAND REMOTE SENSING
1–5 July 2013 | Harokopio University | Athens, Greece

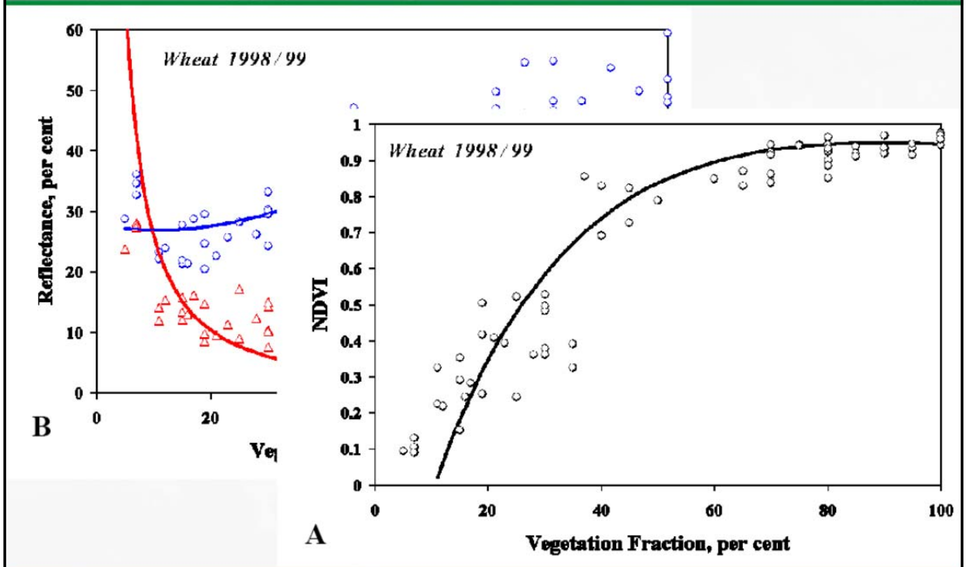

MERIS Terrestrial Chlorophyll Index (MTCI)

$$MTCI = \frac{R_{Band10} - R_{Band9}}{R_{Band9} - R_{Band8}}$$

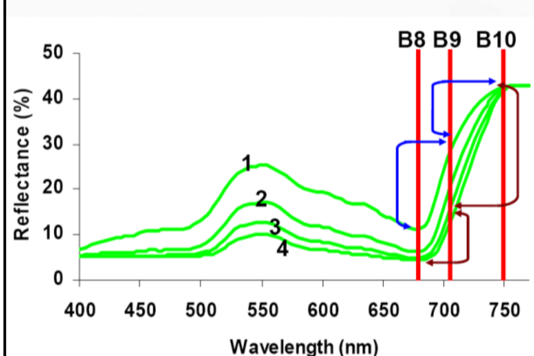

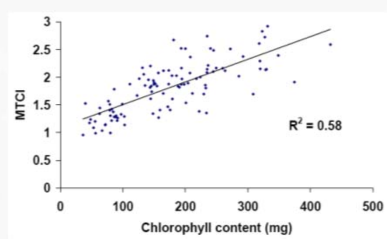

Optimized spectral indices

Leaf chlorophyll

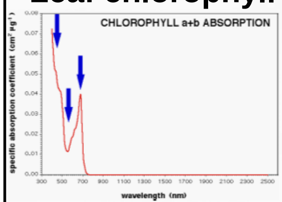

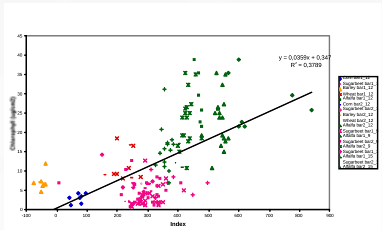

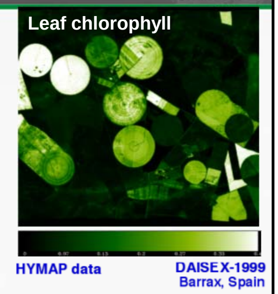

Canopy water

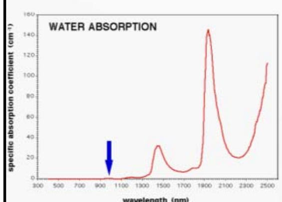

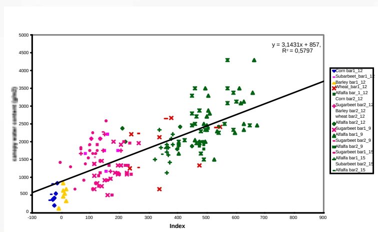

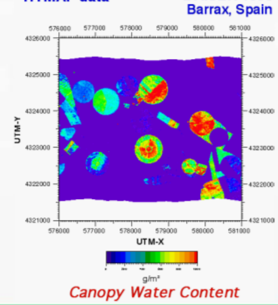

Merit function:

Incorporation of the uncertainties in the inversion process

$\tilde{\rho}_{ij}$ accounts for correlations among different observations

ρ_{ij} accounts for correlations among different biophysical model variables

a priori Covariance Matrix (Observations) — *a priori* Covariance Matrix (Model variables)

$$\chi^2 = \left[R_{mes} - R_{mod}(V)\right]^t W^{-1} \left[R_{mes} - R_{mod}(V)\right] + \left[V - V_p\right]^t C^{-1} \left[V - V_p\right]$$

Residuals — Residuals — Residuals — Residuals

Observations — Model variables

Use of constrained minimization procedures that guarantee the minimal variation of model variables to produce the same output, and a robust initialization procedure of such variables (consistency even if model has global bias).

Neural network methods

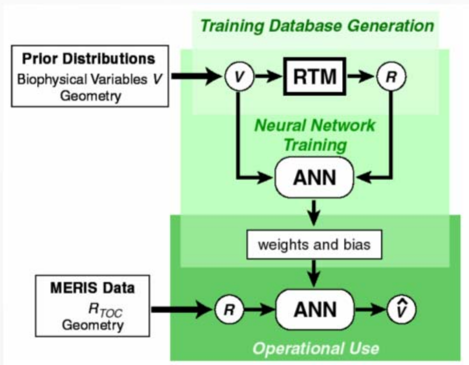

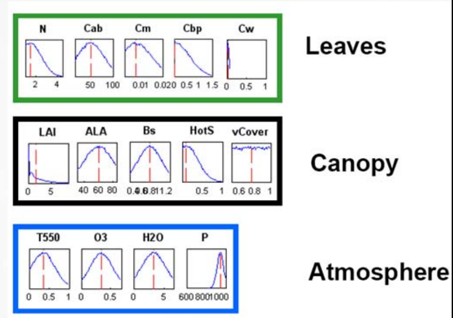

Training becomes the critical issue

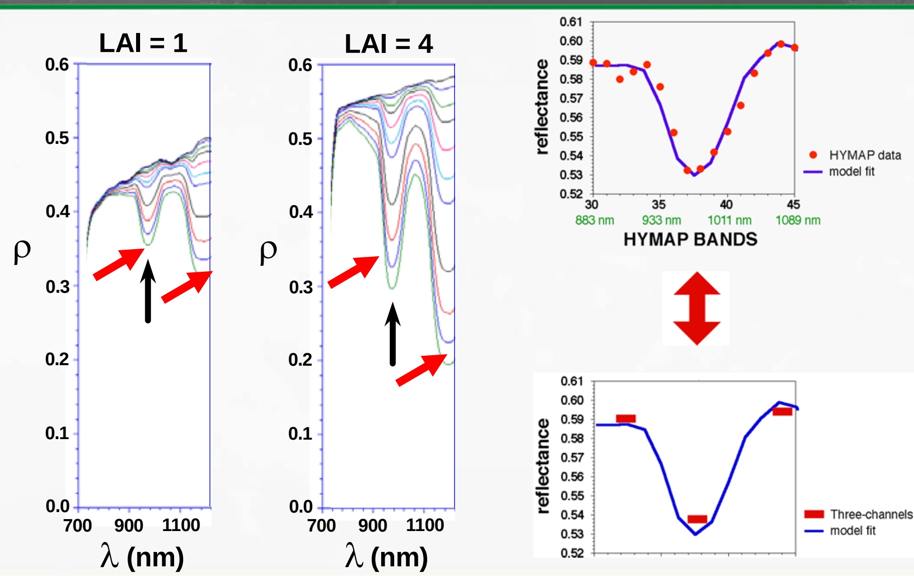

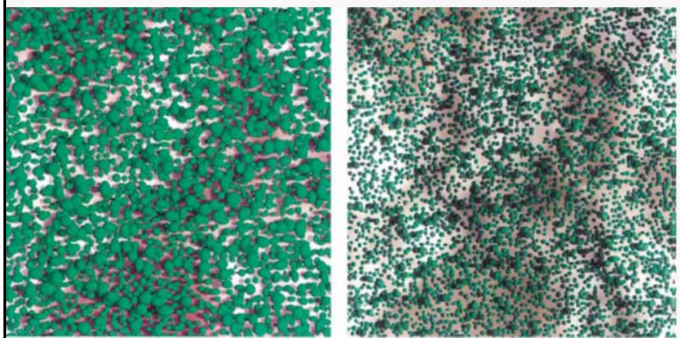

Spatial information in the images

- Textures

- Higher order statistics

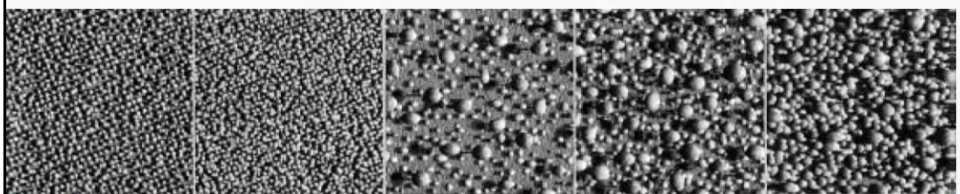

Multiresolution data

VIS/NIR/SWIR Colour Composite **Thermal data**

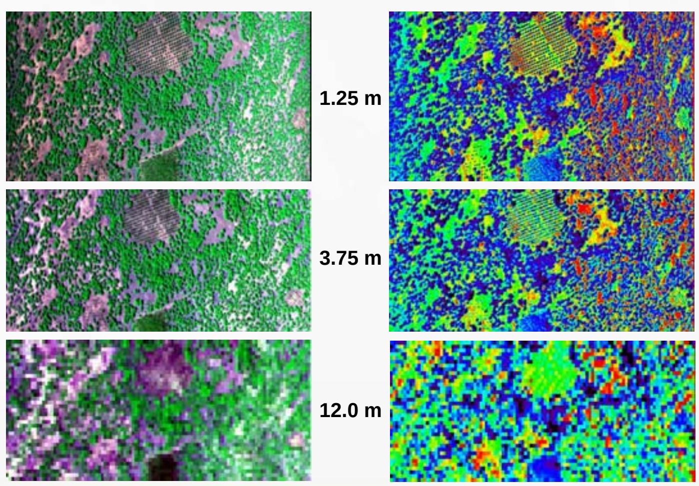

HAROKOPIO UNIVERSITY

esa

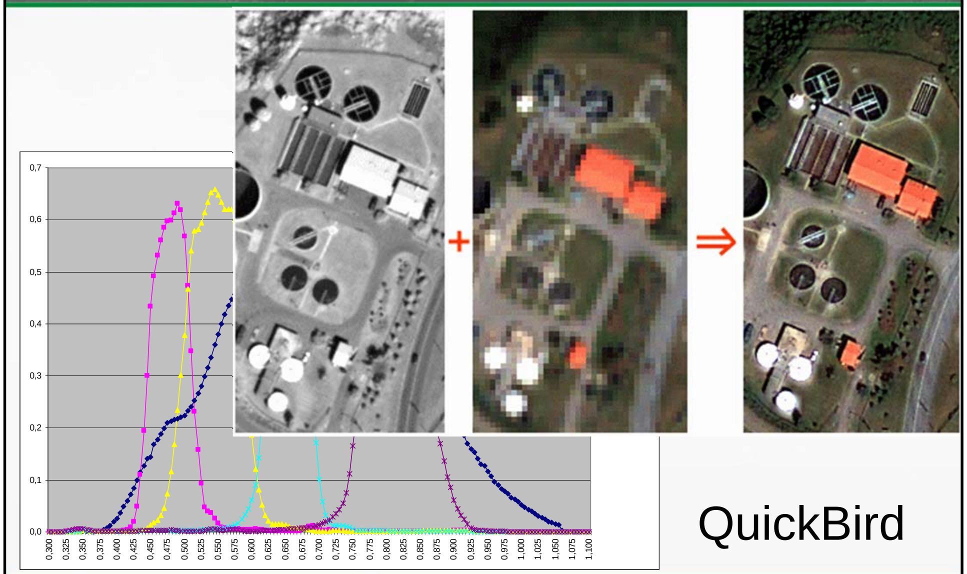

QuickBird

→ 4th ADVANCED TRAINING COURSE IN LAND REMOTE SENSING
1–5 July 2013 | Harokopio University | Athens, Greece

HAROKOPIO UNIVERSITY

esa

counting individual trees by using Quickbird very high resolution imagery

→ 4th ADVANCED TRAINING COURSE IN LAND REMOTE SENSING
1–5 July 2013 | Harokopio University | Athens, Greece

Time series: Coupling canopy functioning and radiative transfer models for remote sensing data assimilation

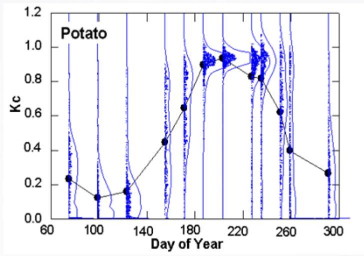

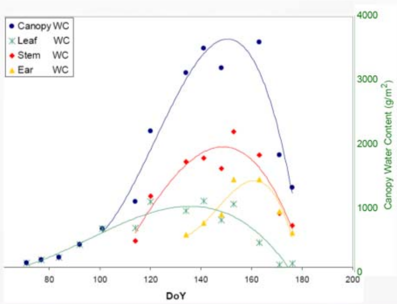

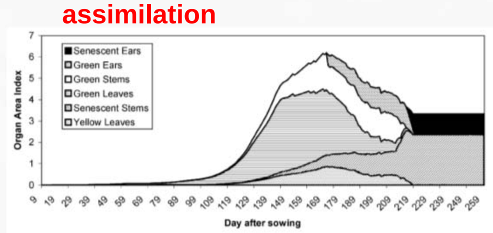

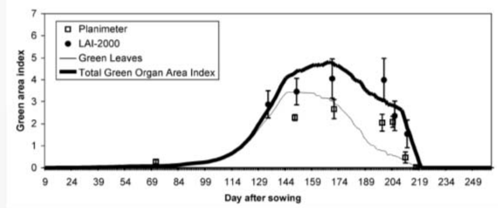

MERIS - 14 July 2003

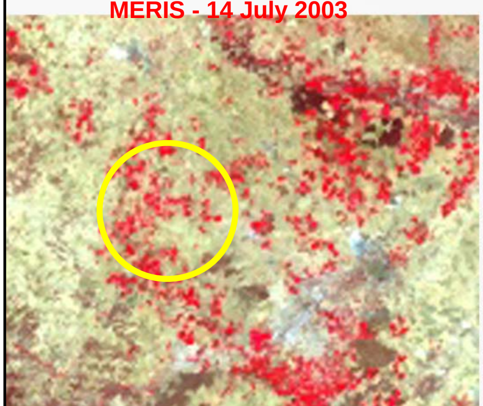

Landsat - 15 July 2003

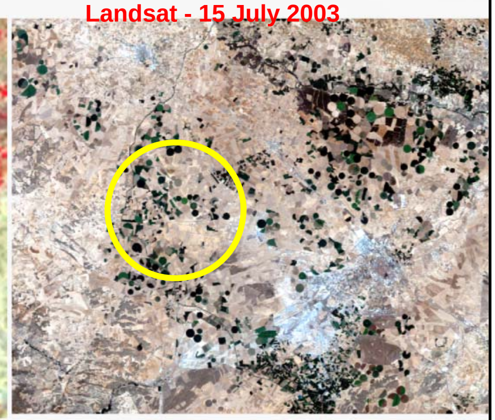

MERIS and Landsat both provide time series at different spatial and temporal scales

HAROKOPIO UNIVERSITY

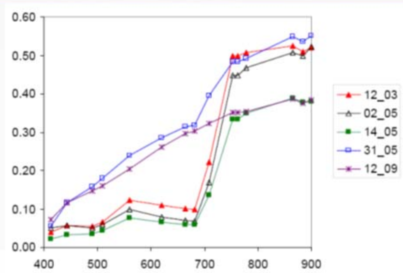

Stable calibration, adequate cloud screening and precise atmospheric corrections are needed for time series analisis

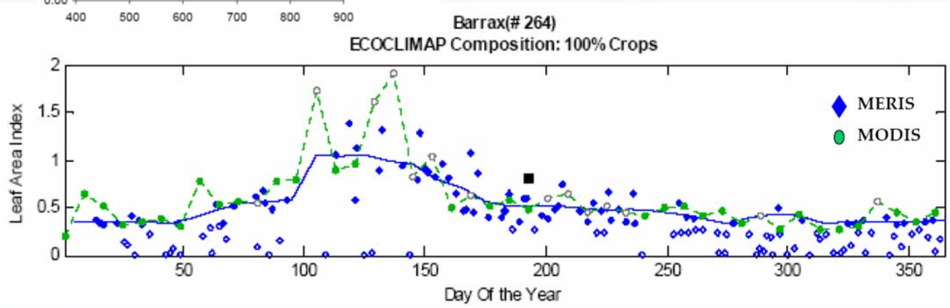

HAROKOPIO UNIVERSITY

ISSUES ABOUT VALIDATION OF RETRIEVALS

- Statistical representativity of measurements used for validation
- Strategy for spatial and temporal sampling
- Validation methodology versus retrieval technique
- Statistical extrapolation of results (sample versus population)
- Adaptation of different methodology for each biophysical parameter
- Examination of results in view of the expected limitations
- Adaptability to the application
- Critical review of actual achievements

Usage of the derived information:

- Tendency: from proxies to quantitative information
- Multi-resolution spatial inputs and time series

- **First approach:** Land cover mapping, classification and tables of biophysical variables assigned to each class
- **Second approach:** Retrievals of biophysical variables as direct inputs to models
- **Third approach:** direct assimilation of radiances/reflectances into models

REMOTE SENSING OF LAND SURFACE PROCESSES

- Mapping Applications
  - cartography
  - thematic mapping
- Monitoring Applications
  - ecosystems dynamics
  - natural hazards (fires, floods, desertification)
- Research about Land Surface Processes
  - heat and mass exchange at Land/Atmosphere interface
  - photosynthesis and net primary production
  - hydrologic processes
  - Land/Atmosphere exchange of biochemicals

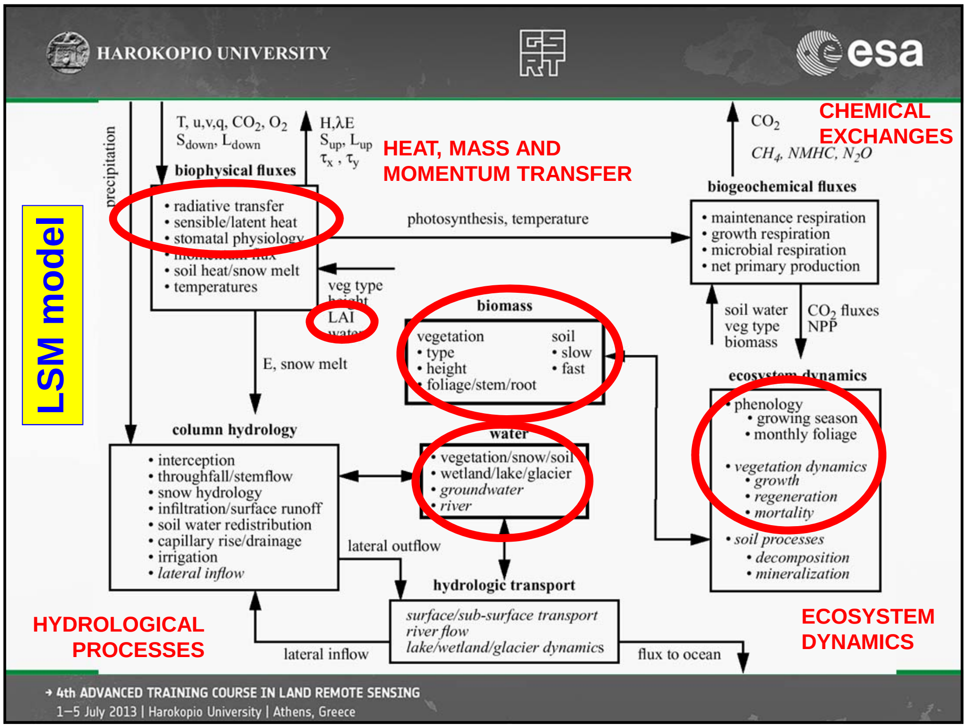
HAROKOPIO UNIVERSITY
esa
LSM model
precipitation
T, u,v,q, CO_2, O_2
S_{down}, L_{down}
H,λE
S_{up}, L_{up}
τ_x , τ_y
HEAT, MASS AND MOMENTUM TRANSFER
biophysical fluxes
• radiative transfer
• sensible/latent heat
• stomatal physiology
• soil heat/snow melt
• temperatures
photosynthesis, temperature
veg type
LAI
CO_2
CH_4, NMHC, N_2O
CHEMICAL EXCHANGES
biogeochemical fluxes
• maintenance respiration
• growth respiration
• microbial respiration
• net primary production
soil water
veg type
biomass
CO_2 fluxes
NPP
biomass
vegetation
• type
• height
• foliage/stem/root
soil
• slow
• fast
E, snow melt
column hydrology
• interception
• throughfall/stemflow
• snow hydrology
• infiltration/surface runoff
• soil water redistribution
• capillary rise/drainage
• irrigation
• lateral inflow
water
• vegetation/snow/soil
• wetland/lake/glacier
• groundwater
• river
ecosystem dynamics
• phenology
• growing season
• monthly foliage
• vegetation dynamics
• growth
• regeneration
• mortality
• soil processes
• decomposition
• mineralization
lateral outflow
hydrologic transport
surface/sub-surface transport
river flow
lake/wetland/glacier dynamics
lateral inflow
flux to ocean
HYDROLOGICAL PROCESSES
ECOSYSTEM DYNAMICS
4th ADVANCED TRAINING COURSE IN LAND REMOTE SENSING
1–5 July 2013 | Harokopio University | Athens, Greece

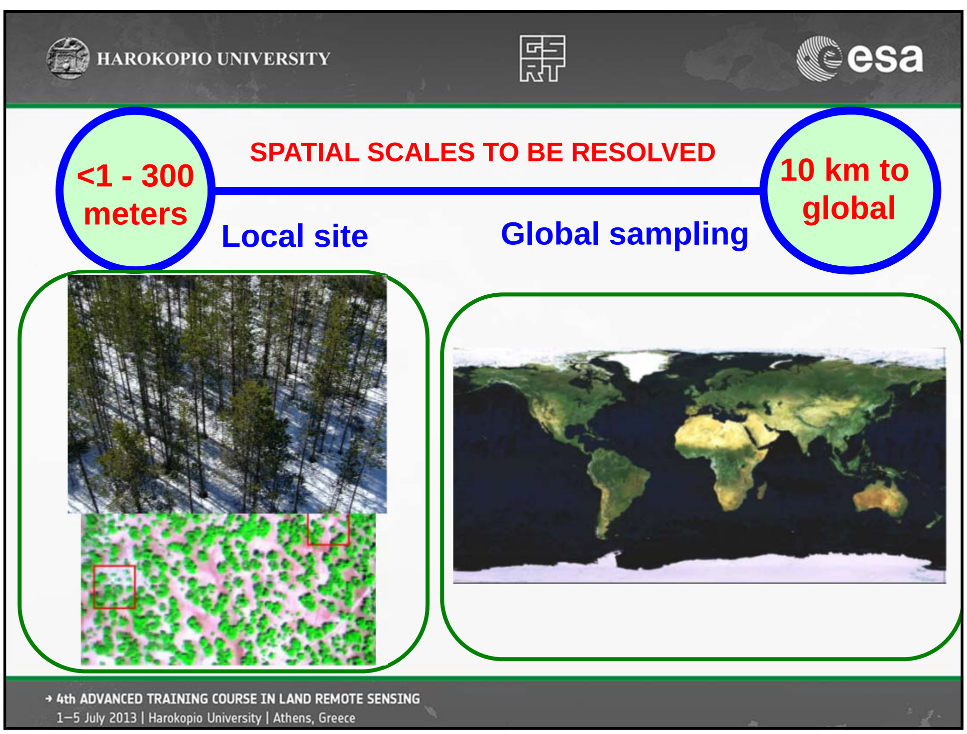
HAROKOPIO UNIVERSITY
esa
SPATIAL SCALES TO BE RESOLVED
<1 - 300 meters
Local site
Global sampling
10 km to global
4th ADVANCED TRAINING COURSE IN LAND REMOTE SENSING
1–5 July 2013 | Harokopio University | Athens, Greece

HAROKOPIO UNIVERSITY

3 - 10 days

TIME SCALES TO BE RESOLVED

> 3 years

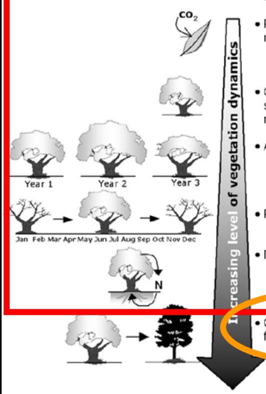

Process modelled	Extent to which vegetation acts as a dynamic component	Timescale at which processes are modelled
• Photosynthesis and leaf respiration.	Stomata responds to variability in environmental conditions and CO_2 concentration when coupling between photosynthesis and stomatal conductance is explicitly modelled.	Minutes to months
• Growth respiration and stem and root maintenance respiration.	Estimating respiration allows us to model NPP. $GPP - R_A = NPP$.	Minutes to months
• Allocation	Biomass allocated to leaves determines LAI. LAI thus varies with change in climatic conditions from year to year, and the seasonal cycle of LAI can be simulated rather than being prescribed.	Daily to annual
• Phenology	The timing of leaf onset and offset is modeled rather than be prescribed.	Daily to monthly
• Nitrogen cycle	Explicitly modeling N cycle and plant N uptake implies that N availability does not have to be assumed constant. The effect of variability in N availability on plant productivity can thus be modeled.	Monthly to annual
• Competition between plant functional types (PFTs).	Vegetation reacts to long-term changes in climate, and PFTs, which are best suited for a given region and climate, succeed.	Decades to centuries

Requires very large time series

→ 4th ADVANCED TRAINING COURSE IN LAND REMOTE SENSING
1–5 July 2013 | Harokopio University | Athens, Greece

HAROKOPIO UNIVERSITY

EO Applications

- Calibration & Validation
- Vegetation monitoring
- Agriculture
- Forestry
- Water quality
- Climate change
- Damage Assessment
- Cartography

Methods

- Physical models
- Instrument design
- Image processing and analysis
- Automatic classification
- Analysis of time series
- Biophysical parameter estimation
- Data fusion

→ 4th ADVANCED TRAINING COURSE IN LAND REMOTE SENSING
1–5 July 2013 | Harokopio University | Athens, Greece

HAROKOPIO UNIVERSITY

NEW GENERATION OF SENSORS

- Well calibrated (more suitable for multitemporal studies)
- Increased spatial resolution (0.5 m PAN now available)
- Increased spatial coverage (global mapping in high spatial resolution (as ESA GMES/Sentinel-2)
- New type of information (i.e., vegetation fluorescence)
- Time series: gap filling using multi-sensor data, better temporal resolution with high spatial resolution
- Integration of multi-resolution data with diverse spectral information in common temporal databases

→ 4th ADVANCED TRAINING COURSE IN LAND REMOTE SENSING
1–5 July 2013 | Harokopio University | Athens, Greece

HAROKOPIO UNIVERSITY

The near future

GMES / Sentinels

→ 4th ADVANCED TRAINING COURSE IN LAND REMOTE SENSING
1–5 July 2013 | Harokopio University | Athens, Greece